Physics, Technologies, and Status of the Wendelstein 7-X Device

F. Wagner, T. Andreeva, J. Baldzuhn, A. Benndorf, H. Bolt, J. Boscary, H.S. Bosch, T. Braeuer, R. Brakel, P. Brand[3)], A. Cardella, M. Czerwinski, C. Damiani[4)], G. Dammertz[2)], A. Duebner, J. H. Ehmler, F. Elio[1)], M. Endler, V. Erckmann, J. Feist, M. Fillunger[5)], G. Gantenbein[3)], W. Gardebrecht, M. Gasparotto[4)], B. Giesen[6)], H. Greuner, H. Greve, P. Grigull, H. Grote, E. Harmeyer, H.J. Hartfuss, D. Hartmann, B. Hein, B. Heinemann, D. Holtum, M. Huguet, F. Hurd, N. Jaksic, W. Kasparek[3)], J. Kisslinger, T. Klinger, J. Knauer, R. Krampitz, H. Laqua, H. Lentz, K. Liesenberg, J. Maier, R. Maix[5)], B. Mendelevitch, G. Michel, M. Nagel, D. Naujoks, H. Niedermeyer, C. Nuehrenberg, A. Opitz, G. Pfeiffer, M. Pietsch, J. Reich, K. Risse, P. Rong, K. Rummel, T. Rummel, C. Sborchia, F. Schauer, R. Schroeder, U. Schultz, S. Schweizer, J. Simon-Weidner, M. Sochor, L. Sonnerup, B. Streibl, J. Tretter, M. Thumm[2)], H. Viebke, M. Wanner, L. Wegener, M. Weissgerber, A. Werner, M. Winkler

1) EFDA, Garching, Germany
2) Forschungszentrum Karlsruhe
3) Institut für Plasmaforschung, Universität Stuttgart
4) Ente per le Nuove Tecnologie, l'Energia e l'Ambiente (ENEA), Roma, Italy
5) Atominstitut der Österreichischen Universitäten, Vienna, Austria
6) Institut für Plasmaphysik im Forschungszentrum Juelich GmbH, Juelich, Germany

Max-Planck-Institut für Plasmaphysik, EURATOM Association, 17491 Greifswald, Germany

e-mail contact of main author: fritz.wagner@ipp.mpg.de

Abstract W7-X is a fully optimised low-shear stellarator of the Wendelstein line. It follows the partially optimised W7-AS device which showed excellent operational characteristics at fusion relevant parameters. W7-X is optimised along the quasi-isodynamic principle. It is built with superconducting coils and ECRF heating and plasma exhaust are developed for 30 min operation. At present, the device is at the transition from component procurement to assembly. W7-X has a high ITER relevance and it represents an excellent training bed for European industry.

1. Introduction

Stellarators belong to the family of toroidal confinement systems. Their confinement is achieved by external means, by currents in external conductors. Toroidal equilibrium in external confinement systems is only possible in 3-dimensional flux surface geometry. The lack of continuous symmetry in the magnetic field gives rise to high collisionless orbit losses with the consequence of intolerably high neo-classical fluxes under reactor conditions and insufficient α-particle confinement. Because of the large aspect ratio of low-shear stellarators, the equilibrium is characterised by a large Shafranov shift.

W7-AS (terminated mid-2002), the predecessor of W7-X, was a medium-sized, low-shear, advanced stellarator with modular coils, which produced simultaneously the poloidal and toroidal field components by one set of non-planar coils. W7-AS did not represent a classical stellarator as its field was partially optimised with a reduced factor of $\langle j_{\|}^2/j_{\perp}^2 \rangle$ giving rise to improved equilibrium with a Shafranov shift reduced by a factor of 2 in comparison to a classical ($l = 2$) stellarator.

W7-AS was operated with an island divertor in its last phase and demonstrated its capabilities along with 3-D modelling of the scrape-off-layer. The divertor concept is based on the natural island chain, which develops at the edge owing to the five-fold toroidal symmetry when $\iota/2\pi = 5/8$, 5/9, or 5/10 is selected at the edge. W7-AS with island divertor showed excellent plasma performance with confinement in the H-mode, high density operation up to $n_e = 4\times10^{20}$ m^{-3} (2.5 T) and $\langle\beta\rangle$ up to 3.4 % (0.9 T). Towards high density, a specific form of the H-mode developed, the high-density H-mode (HDH-mode), which had excellent energy and low impurity confinement and did not show ELMs (easing exhaust conditions). The MHD spectrum of W7-AS showed beam and thermal pressure driven instabilities (global Alfven eigenmodes, MHD modes linked to rational ι-values and ELMs in the standard H-mode. Towards high β, close to operational boundaries, all modes disappeared and plasmas became rather quiescent owing to a diamagnetically deepened magnetic well. High-β plateaus could be operated up to 65 confinement times with good confinement: $\tau_E/\tau_{E\ ISS\text{-}95} = 2$ /1/. Such

discharges – when characterized by tokamak operational factors – had: $q = 2$; $n_e/n_{GREENWALD} = 3$; $\beta_N = 8.5$. Results from W7-AS are summarized in Ref. /2/.

2. The Wendelstein 7-X design principles

The Wendelstein 7-X /3/ device will follow W7-AS. It is a large optimised superconducting stellarator with 50 modular coils and 20 planar coils. ECRH and exhaust are designed for 30 min. operation. W7-AS and W7-X share the 5-fold toroidal symmetry, the low-shear characteristics to avoid low-order rational ι-values in the gradient region, and a poloidal cross-section formed from multiple helicities (l=2, l=3). W7-AS and W7-X differ in the magnetic axis, which is planar in case of W7-AS and helical in W7-X. Thus, W7-X is centred around $\iota/2\pi = 1$ ($0.72 < \iota/2\pi < 1.25$) whereas W7-AS operated in the range $0.2 < \iota/2\pi < 0.6$). The major conceptual difference is that W7-X is fully optimised following the quasi-iso-dynamicity principle /4/. This concept recognises that particle orbits in a 3-D magnetic field - if expressed in appropriate magnetic coordinates (Boozer coordinates) - depend on the field strength |B| only. |B| can be made symmetric, and, subject to a constant of motion, particle orbits are closed. Quasi-isodynamicity addresses the property that trapped particle gyro-centres located in the straight sectors of the pentagon precess poloidally with the confinement of thermal and energetic particles ensured by poloidally closed contours of the second adiabatic invariant.

The optimisation of W7-X leads to:

- good and nested flux surfaces,
- low Shafranov shift thanks to a ratio of $\langle j_{\|}^2/j_{\perp}^2 \rangle \sim 0.5$, which is further reduced in comparison to W7-AS,
- equilibrium and stability $\langle\beta\rangle$ of 5 %,
- low neoclassical fluxes with a confinement determined by turbulent transport,
- small bootstrap current to maintain the optimised characteristics toward high-beta.
- Edge-island chains as basis of the island divertor (based on 5/5 (standard), 5/4 (high iota) or 5/6 low iota) cases).

Technically, both W7-AS and W7-X are designed for 2.5 T and employ 140 GHz ECRH as fundamental plasma heating. The major technical and geometrical advancements from W7-AS to W7-X are given in Table 1:

	W7-AS	**W7-X**
Major radius R_o (m)	2	5.5
Minor effective radius a_{eff} (m)	0.18	0.55
Plasma volume	1.3 m^{-3}	30 m^{-3}
Number of non-planar coils / conductor	45, Cu	50; NbTi
Number of planar coils / conductor	10; Cu	20; NbTi
Pulse length	10 sec	30 min
Heating power (ECRH, NBI, ICRH)) (MW)	2.5, 3, 1	10, 5 (20*), 3 (9*)
Energy turn around	5. MJ	1.8 GJ

* stage II heating

The goals of W7-X are to explore the suitability of the inherent optimisation for a stellarator power plant. W7-X will operate with hydrogen and deuterium and it will operate in reactor-like collisionality and beta ranges. Apart from the proof that the optimisation works as foreseen, W7-X will address the important questions of thermal and beam driven instabilities under optimised conditions, turbulent transport with particle orbits close to the flux surface, and impurity transport at high density. Impurity transport is an extremely important question for steady-state plasma operation and specifically for stellarators facing their inherent tendency to impurity accumulation at high densities. Therefore, an important question on concept and the level of heating power is whether the HDH threshold conditions can be met to prevent impurity problems and allow for steady-state operation close to operational boundaries. W7-X will further develop the island divertor and will address the

programmatically important issues of plasma-wall interaction in long plasma pulses (recycling, erosion, inventory).

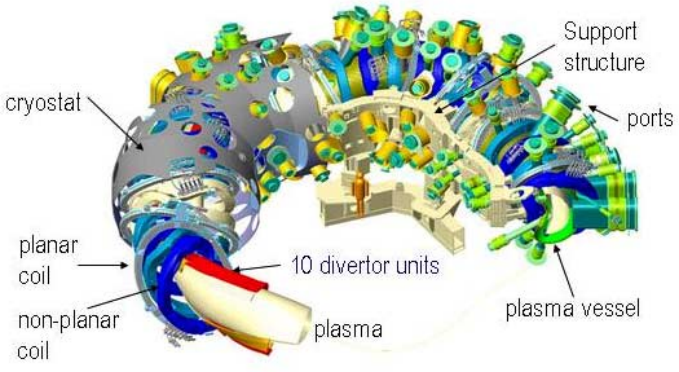

Fig. 1. Components of Wendelstein 7-X.

W7-X will start operation in 2009/10. It will provide data and operational characteristics which have to be compared with those from LHD /5/ and NCSX /6/. These two devices belong to the family of helical systems but they are based on different concepts: LHD is a heliotron with superconducting coils operating since 1998 and NCSX is also an optimised system following the line of quasi-axi-symmetry /7/. NCSX will have copper coils and the device should start in 2007. These three devices will ultimately provide the database to decide upon the helical concept with the best reactor prospects. This development will be in parallel to that of ITER so that, at the end, a large database will be established for a decision on the concept of DEMO. This decision has to differentiate between the geometrical complexity of a three-dimensional system, which provides continuous and quiescent plasma operation and geometrical simplicity necessitating, however, additional external means to provide steady-state operation, the proper current profile and suppression of current-driven modes.

3. Components of W7-X

Fig. 1 shows a CAD drawing of W7-X. The technical development and the design principles of the major components of W7-X are described in recent publications /8/. In this paper we will concentrate on a few relevant topics.

3.1. Non-planar coils

The 50 non-planar coils establish the basic magnetic confinement system. It is set-up by 5 differently shaped coil types. The winding pack is built from a NbTi conductor. It is embedded in a welded casing made out of cast-steel using quartz sand and epoxy. Up to now, 4 coils have been tested at CEA in Saclay, 37 winding packs are built and 17 coils are in different stages of assembly.
The following comments should be made:

- All cast coil casings have to be X-rayed because of the wall thickness by linacs or betatrons.
- The contact areas between coil casings and inner support ring and between neighbouring non-planar coils require a careful final machining to meet the stringent mechanical accuracies. Specifically critical is the inner toroidal circumference where the coils are separated by small gaps only and, after contact, large and variable forces are transmitted.
- It was necessary to go through a detailed qualification process for the quench detection wire including low temperature tests and tests at reduced gas pressures. At a quench, the coil system has to be discharged with a time constant of about 3 sec. Maximal high voltage is 8 kV. The final design uses Kapton insulated wires enclosed by a metallic shield.
- The accuracy and reproducibility of the physical dimensions of the winding packs meet the specified constraints. Most critical are perturbations of the field, resonant with $\iota/2\pi=1$, which can change the geometry of the edge islands, increase the level of stochasticity at the X-points, introduce additional magnetic islands and lead to the asymmetric power load onto the target plates. The geometry of each winding pack is described by 96 poloidal cross-sections. The actual measures are compared with the ideal CAD model via a best-fit approach.

Fig. 2 shows the systematic and random deviations for seven coils of type 1 determined by this procedure. The systematic deviation maintains the system symmetry and can be neglected. The requirements of reliable divertor operation limit the relative amplitude of error field components, caused by the random deviations to $\Delta B/B_{00} \leq 2 \cdot 10^{-4}$, where B_{00} is the average field strength on the magnetic axis and $\Delta B = \sqrt{(B_{11}^2 + B_{22}^2 + B_{33}^2)}$.
The current status of the coil fabrication is that the average absolute deviations for already manufactured winding packs with respect to the CAD model are < 3 mm, and their average relative deviations with respect to the average shapes of each coil type are < 2 mm. Expectation of the perturbed magnetic field by the completion of all winding packs is $\Delta B/B_{00} \sim 1 \cdot 10^{-4}$. The remaining margin to the permissible limit serves as a guideline for the assembly accuracy requirements to be discussed in chapt.4.

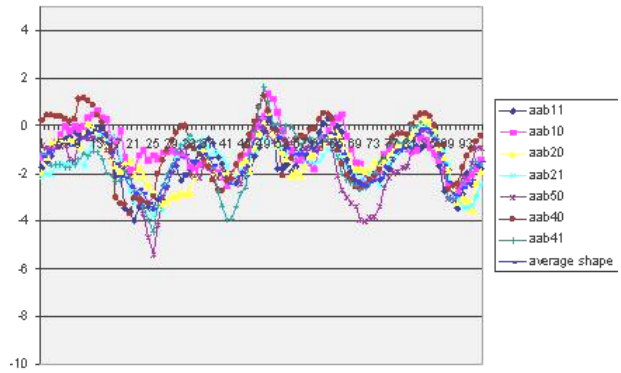

Fig.2 Manufacturing deviations of seven coils of type 1 (inner contour). Ordinate scale is mm.

In case that the maximal error field is exceeded, main resonant Fourier harmonics can be corrected by additional coils. The divertor (control) coils are separately energised and can correct mainly B_{33} and B_{44} components since they are located close to the plasma surface. However they have a low capability with respect to the B_{11} and B_{22} Fourier components. Space for a set of 5 steady-state copper coils on top of the outer vessel is reserved, which would allow the correction up to B_{11}/B_{00} of $4 \cdot 10^{-4}$. These coils will be realised only when needed.

All coils are subjet to a test at operational conditions at CEA in Saclay. The test procedure for the superconducting non-planar coils foresees a complete quench at nominal current in the self-field of the coil at specified He-flow rate (3.6 g/sec). The quench-conditions are approached in temperature steps of 0.1 K; stable conditions are developed prior to the next step in temperature. In an additional test step, the coil is kept just below the quench temperature (safety margin test) for 30 min. The critical conditions (35 kA) at 4.0 K and 6T translate to 5.7 K in the self-field of 17.6 kA. In all tested cases up to now, the quench temperature was above 6 K, which represents some additional margin. Fig 3 shows a test cycle where the temperature was increased in steps; the quench occurred at 6.1 T. The critical currents compare well with the properties of the single superconducting strands. Other tests, which the coils have passed are the flow rate at specified pressure difference, high-voltage tests and deformation tests when energized; the deformations show a quadratic dependence on current.

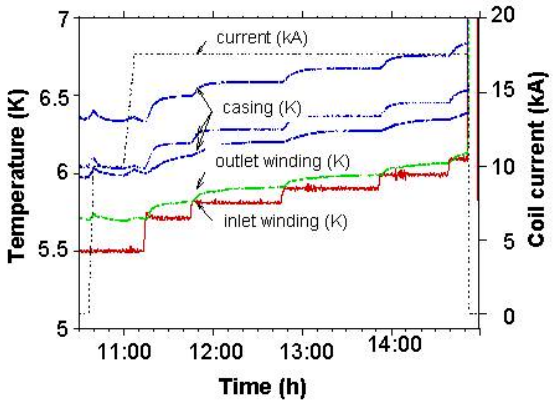

Fig. 3. Temperature and current signals during current quench test.

3.2. Planar coils

Three coils have been cryo-tested in Saclay; 17 winding packs are fabricated; 10 coils are in various stages of assembly. All winding packs are fabricated with sufficient accuracy; all three coils have passed the cryo-test, which is the same as that for the non-planar coils.

3.3. Magnet support system

The coil support structure of W7-X is rather complex because it is the result of a compromise which provides the integrity of the magnet system (viz. limited deformations with acceptable stresses) under the flexible conditions of an experiment with additional installations like the planar coils to vary iota or the large number of ports for heating and plasma diagnostics, which restrict the available space.
The central coil forces are backed by a central support ring; the connections are done via central support elements (see Fig. 4). Between the non-planar coils support is provided by the so called narrow- gap-elements on the high-field side and the lateral-support-elements on the low-field side. Planar-support-elements connect the planar coils with the non-planar coils. The design of the various support components is done as a compromise between tolerable deformations and allowable stresses. The results are based on a global FE model employing the ADINA code. Central and lateral supports are realised as firm connections (bolted or welded), the narrow-gap and the planar-support-elements as contact elements, which allow the components to slide and tilt.

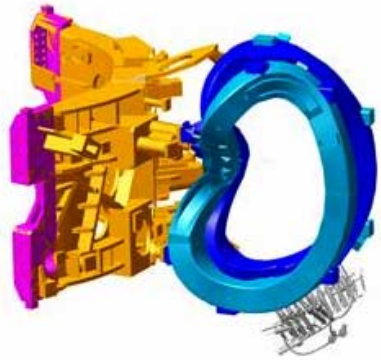

Fig. 4 Modular coils mounted onto the coil support ring.

The most critical connection are the narrow-gap-elements, which consist of pads (Al-bronze, ~ 65 mm Ø, 18 mm thickness) with slightly spherical surfaces to allow sliding (up to 2 mm) and tilting (up to 0.5°) movements of the coils. These pads are kept by a pad frame on one coil and a sliding surface on the other casing. The frame contains a spring which keeps the pad centred. Without coil current there are gaps between 0 to 4 mm between pad and the adjacent coil in order to optimise the load distribution among the narrow supports. These gaps close when the coils are energized; ultimately, forces of up to 1.1 MN build up. In order to allow for coil movement without jerks, the pad is covered by a MoS_2 lubricant layer which itself is protected by a SiO_2 layer. Room-temperature tests on air have confirmed the viability of this concept with forces of 1.5 MN for 1500 cycles. Low temperature tests in vacuum are in progress.

3.4. Bus system

The bus system, developed by Forschungszentrum Jülich, establishes the superconducting current connections between the superconducting coils and between the coils and the current supply terminals. The bus lines are routed bifilar to minimize field perturbations. The complicated assembly is optimised by using a 1:1 model. Insulation checks include Paschen-tests; also the quench situation will be studied.

3.5. Plasma Vessel

Fig. 5 Thermal insulation mounted onto one vessel half-module sector.

The plasma vessel is matched to the 3-D shape of the plasma. It is formed from 200 welded steel rings and split into 10 sectors each again is split into 2 sectors to allow the assembly of the first coil. The vessel can be cooled or heated (to 150 °C). The vessel sectors for one module are delivered to Greifswald.

3.6. Thermal insulation

Three regions with different conditions have to be discerned for thermal insulation: The plasma vessel, the outer vessel and the ports. In all cases

the insulation consists of multi-layer insulation (MLI) and an actively cooled thermal shield. The coil and coil support cooling system is designed for a maximal heat influx from the shields of 1.5 W/m^2. The thermal insulation of one plasma vessel sector is finished. This is the first needed and technically the most demanding part. It is shown in Fig. 5.

Each plasma vessel half-module (HM) insulation is built up from twenty thermal shield panels with corresponding MLI panels attached to them. Each shield panel is cooled by two tubes. For adaptability to the complex plasma vessel surface and for heat resistance, aluminized crinkled polyimid (Kapton) foils with glass fabric in between was chosen. The MLI panels are built up from two shifted mats of ten layers each for simple overlap between panels. Tests of such a 20-layer MLI system under realistic and compressed conditions resulted in low losses of 0.93 W/m^2.
The thermal shields are made out of laminated epoxy-glass resin panels containing three copper meshes for thermal conductivity. They are cut into two or three electrically insulated parts each in order to reduce eddy currents. FEM analysis and accompanying tests confirmed their thermodynamical, electrodynamical and mechanical behaviour. The radiation emissivity of the panel surface facing the cold coils is reduced by applying adhesive aluminium tape.

4. Assembly

The assembly of W7-X is split into 5 major phases /9/. In the first phase, half modules comprising a tenth of the magnet system are assembled in two assembly stands. A half module consists of the plasma vessel, the inner thermal insulation, 5 non-planar and 2 planar coils and one tenth of the central support ring. In the second step, the two flip-symmetric half modules are connected in the second assembly stand to a module. Bus-bar system and He-piping are added. Thereafter, the module is moved onto assembly stand 3 which is equipped with the lower half shell of the outer vessel. The module is lowered into the outer vessel sector and firmly connected. This unit is then moved onto its position on the experimental platform and completed with the upper half of the outer vessel, the ports and the plasma facing components. In the fifth step, the five modules are precisely adjusted to minimise the overall field error; periphery is added and the device is connected to the external supplies.
The major challenges as seen at present are as follows:
- A vessel half-module is split into two pieces to allow the assembly of the first coil. After this is done, the two vessel pieces are welded. The tolerance range for this process is 3 mm around the ideal surface of the CAD model. A trial welding has shown that this accuracy can be met.
- The 6 t coils have to be positioned to an accuracy of about 1 mm. The assembly accuracy is monitored by laser tracker. Assembly trials have shown that this accuracy can be met.
- Detailed numerical studies and assembly trials are carried out to ensure beforehand collision-free paths for the coils to their final positions, for the 299 ports, which are radially moved from the outside through the cryostat to their final position, and for the bus-bar system comprising of 25 individual conductors per module.
- To ensure leak-tightness of all welds, which generally are along non-standard contours.
- The insertion of the narrow-support elements in a tight space with restricted accessibility.
- The maintenance of the maximally tolerable field error during assembly. The connection of the five modules to a toroidal coil system offers the last possibility to correct the then known errors of the individual modules. The positioning of the modules will be accompanied by field calculations so that the final module placement minimises the overall error. The position of the modules can be varied by 5 mm. Sensitivity studies are underway.

Half-module assembly has been started. The vessel pieces of the first module have been equipped with diagnostics (saddle coils) and the assembly of the thermal insulation has started. The first coils will be mounted beginning of 2005. Up to this date, the training of coil assembly and the studies of the assembly technology of the various support elements will continue.

5. The ITER relevance of W7-X

W7-X is the last large superconducting device to be built in Europe before the start of ITER and it serves to train European industry in fusion technology and the required level of documentation and quality assurance.
Whereas the physics basis for ITER is well developed there is a need on steady-state operational experience, plasma control and diagnostics, and on long-pulse technology, specifically heating and exhaust. In Europe, W7-X will continue the work done with Tore-Supra and it will be operated together with the other long-pulse superconducting devices LHD, KSTAR, EAST and SST-1.
Two examples should demonstrate the role, W7-X plays already now for the development of ITER.

5.1 ECRH system

A 10 MW cw ECRH system operating at 140 GHz will provide the fundamental heating of W7-X, especially for its major scientific objective - the demonstration of steady-state operation at reactor relevant plasma parameters. The ECRH system is being developed and built by FZ Karlsruhe (FZK) as a joint project with IPP and IPF Stuttgart. The modular design of the ECRH system comprises 10 units with 1 MW each. A W7-X prototype gyrotron with 1 MW output power has been developed in collaboration with European research laboratories and industries (TED, France) /10/. The pre-prototype gyrotron "Maquette" which does not completely meet the full power, cw specifications is operational at Greifswald and is presently used for high power, cw tests (few minutes) of the transmission system and other critical components. Its operation also demonstrated the integrated functioning of all auxiliary systems like the first HV-power supply unit (65 kV, 50 A), gyrotron and transmission line cooling, cryogenic supply, central control system and network.
The second cw gyrotron in operation in Greifswald is supplied from the U.S company CPI and is in the conditioning phase. The data achieved up to now are 600 kW for 5 min, 700 kW for 40 s, processing is done at 830 kW presently.
The second R&D prototype gyrotron from TED has been successfully tested at FZK with an output power of 0.89 MW for three minutes (test stand limit) and 0.54 MW for about 15 minutes. Delivery of the first of 7 series tube from TED is scheduled for Dec. 2004.

The ten gyrotrons at Greifswald will be arranged in two subgroups symmetrically to a central beam duct in the ECRH hall. The RF-beams of each subgroup are combined and transmitted by a purely optical multibeam waveguide (MBWG) transmission line of typical 50 m length from the gyrotrons to the torus. The combination of the five gyrotron-beams to two beam lines with a power of 5 MW each reduces the complexity of the system considerably.
For each gyrotron, a matching assembly of five Single-Beam Waveguide mirrors (SBWG) is mounted on a common base frame. Two phase correcting mirrors match the gyrotron output beam to the stigmatic Gaussian beam with the correct beam parameters, two others are used to set the appropriate polarisation needed for optimum absorption of the radiation in the plasma. A fifth mirror directs the beam to a plane mirror array (beam combining optics unit), which is situated at the input plane of the MBWG /11/. A newly designed short-pulse calorimeter (< 0.5 s) is installed on each SBWG-frame for absolute calibration of the gyrotron output power. The MBWG is designed to transmit up to seven beams from the gyrotron area (input plane) to the Stellarator hall (output plane). It consists of 4 focusing mirrors in a confocal arrangement plus additional plane mirrors to fit the transmission lines into the building. The configuration of the mirrors is such that mode conversion, which is a general feature of curved surfaces, cancels at the end of the MBWG. Additionally, distances and focal lengths for each beam path are designed to achieve a geometric-optical imaging from the gyrotron output to the torus windows, which makes the system insensitive to misalignment.
At the output plane of the MBWG, a mirror array separates the beams again and directs them through diamond vacuum barrier windows to the in-vessel front steering launcher.

The entire transmission-system was tested on the low-power test facility at the IPF and shows an efficiency of 90±2 % in good agreement with the calculations of the transmission properties (92%).
The installation of all SBWG-mirror modules as well as the MBWG-mirrors is completed in the beam duct. Two beam lines are presently under high power, cw test. For long-pulse (> 0.5 s) operation the beam is steered into a commercial cw microwave-load.
The MBWG system could easily handle more than twice the rf-power due to the low power density on the mirror surfaces, which is compatible with the ITER demand.

5.2. Plasma-Facing-Components

Like W7-AS, W7-X will have 2×5 divertor modules /12/ placed at the bean-shaped poloidal cross-section. They comprise target and baffle plates. The target plates (19 m^2), which are formed by 890 elements, are made from flat CFC tiles bounded to the CuCrZr cooling structures bonded with a copper interlayer to the cooling structure. Four cooling channels, equipped with swirl tapes, provide a sufficient heat exchange for the expected target load. (For W7-X, the mono-block concept has been discarded mainly due to geometrical problems.) Target plates are designed for 10 MW/m^2 steady-state heat fluxes. The baffle plates (33 m^2) form a somewhat closed divertor chamber to increase pumping efficiency. They are made out of flat fine-grain graphite tiles (~2900 elements) screwed onto CuCrZr cooling structures. They are designed for up to 0.5 MW/m^2.
The wall protection is split into the protection of the high-field side (45 m^2, ~3400 graphite tiles) and the low-field side (70 m^2; B_4C coated stainless-steel panels).
The design of all protection areas is finished. Prototypes of target elements have been successfully tested up to 12 MW/m^2 steady-state and 15 MW/m^2 for short pulses. The critical heat flux is expected to be ≥ 25 MW/m^2. The baffle plates and wall protection panels have passed the critical test under maximal operational conditions. Also the B_4C coating programme has successfully be finished in co-operation with industry. All plasma facing components are in industrial fabrication. A high heat flux test stand has been built in Garching to qualify the series production of target elements. This ion beam facility can also be used for PFCs of ITER. Irrespective of the detailed design, the industrial experience with series production and that of non-destructive examination of complex compound structures as employed for PFCs is of high relevance for ITER.

References

/1/ U. Stroth, et al., Nucl. Fusion 36, 1063 (1996).
/2/ Proceedings of the 14th Intern. Stellarator Workshop in Fusion Science and Technology, 46, No. 1 (part 1) and No. 2 (part 2).
/3/ M. Wanner et al. Nucl. Fusion 43, 416 (2003).
/4/ J. Nührenberg et al., Transactions of Fusion Technology, 27, 71 (1995)
/5/ O. Motojima et al., this conference.
/6/ M.C. Zarnstorff et al., Plasma Phys. Contr. Fusion, 43:12A, 237 (2001).
/7/ J. Nuehrenberg, et al., E. Sindoni, F. Troyon and J. Vaclavik (Eds.), SIF, Bologna 1994, p. 3.
/8/ J.-H. Feist et al., Fusion Science and Technology, 46, 192 (2004).
M. Gasparotto et al., SOFT Conf., Venice, 2004, paper IN-184.
/9/ L. Wegener et al., SOFT Conf., Venice, 2004, paper I6.
/10/ G. Dammertz et al., IEEE Trans. Plasma Science **30,** 808 (2002).
/11/ L. Empacher et al., in Fusion Technology 1996, Elsevier Science B.V. Amsterdam (1997), 541-544.
/12/ H. Renner et al., Fusion Science and Technology **46**, 318, (2004).